Sensors and Materials, Vol. 37, No. 4 (2025) 1471–1489
MYU Tokyo

S & M 3999

Spatiotemporal Characteristics and Applicability of Energy Consumption Carbon Emissions and Vegetation Carbon Flux in Beijing

Shuang Wu,[1,2*] Yuan Zhuang,[1] Yutao Huang,[3]
Xiaohui Bai,[1] Bogang Yang,[1,4] and Tiantian Yu[1,4]

[1]Beijing Institute of Surveying and Mapping, No. 60, Nanlishi Road, Xicheng District, Beijing 100045, China
[2]Beijing Key Laboratory of Urban Spatial Information Engineering, No. 60, Nanlishi Road, Xicheng District, Beijing 100045, China
[3]Heilongjiang Province Key Laboratory of Geographical Environment Monitoring and Spatial Information Service in Cold Regions, Harbin Normal University, Harbin 150025, China
[4]Beijing Society of Surveying and Mapping, No. 15, Yangfangdian Road, Haidian District, Beijing 100038, China

(Received September 24, 2024; accepted April 11, 2025)

Keywords: energy consumption carbon emissions, vegetation carbon flux, carbon neutrality

The reduction of energy carbon emissions and the increase in the number of vegetation carbon sinks play a crucial role in achieving China's "carbon neutrality". As a megacity, Beijing faces significant pressure to reduce carbon emissions and increase the number of carbon sinks because of its large number of individual buildings, high population density, overcrowded transportation, and enormous amount of human activity. Therefore, calculating and analyzing the carbon emissions, vegetation carbon flux, and spatial distribution in Beijing in recent years provide data that support energy conservation and emission reduction, urban fine management, ecological security pattern planning, and national land spatial planning, and contribute to the high-quality development of the capital. In this study, we applied the C-FIX model, referring to the "2006 IPCC National Greenhouse Gas Inventory Guidelines" and the "Provincial Greenhouse Gas Inventory Compilation Guidelines" compiled by China. The statistical yearbooks of different administrative regions in Beijing were referred to in calculating the energy consumption carbon emissions and vegetation carbon flux of Beijing in 2010 and 2020. The results show the following: 1) In 2020, the carbon emissions from energy consumption decreased by 36.78%, with the reduction of industrial energy consumption emissions playing a major role. 2) The demand for energy in residents' daily lives significantly increased from 2010 to 2020, with the majority of the increase concentrated in areas with larger populations and more frequent activities. 3) Forest land in urban centers mostly serves as a carbon source, while in suburban areas, it serves as a carbon sink. The carbon flux of forest land in most areas shows an increasing trend, and the overall quality of forest land is good. 4) Grasslands in urban areas mostly serve as carbon sources, while those in suburban areas serve as carbon sinks. Moreover,

*Corresponding author: e-mail: 317643852@qq.com
https://doi.org/10.18494/SAM5378

ISSN 0914-4935

the carbon sink capacity in most areas decreases, resulting in poor grassland quality. 5) The carbon absorption by vegetation is lower than the carbon emissions of energy, but the gap is significantly reduced.

1. Introduction

The IPCC Sixth Assessment Report stated that the concentration of carbon dioxide (CO_2) in the atmosphere had reached 409.9 (±0.4) ppm by 2019, an increase of 125 ppm compared with that in 1850.(1) The significant increase in the concentration of atmospheric greenhouse gas emissions caused by human activities was the main factor behind climate warming.(2) As an important carrier of human production and life, cities have become the main source of global carbon emissions and the main contributor to climate change.(3–5) The impact of urbanization on urban carbon emissions continues to increase. At the 75th United Nations General Assembly, General Secretary Xi Jinping pledged that China aims for its carbon dioxide emissions to peak before 2030 and strives to achieve the ambitious goal of carbon neutrality before 2060. This means that carbon dioxide emissions per unit of gross domestic product (GDP) in 2030 will be reduced by 60 to 65% compared with those in 2005. Under the advocacy of the Paris Agreement and the United Nations 2030 Agenda for Sustainable Development, low-carbon and sustainable development research had attracted increasing attention from the academic community.(6–8) At the same time, urban expansion and rapid development have promoted the rapid development of urban infrastructure and construction, and energy consumption has increased rapidly, making China the world's largest carbon emitter.(9) Energy carbon emissions, the vegetation carbon budget, and the impact of land use change on the carbon budget have become important topics in current carbon emission research.(10–13)

As a megacity, Beijing has a large number of individual buildings, a high concentration of population, dense traffic, and an enormous amount of human activity that lead to an increase in carbon emissions year by year and is still facing great pressure to reduce carbon emissions and increase the number of carbon sinks. In the "Beijing Urban Master Plan (2016–2035)", it was proposed to improve the overall environmental quality of Beijing by 2020, further enhance a green, low-carbon lifestyle, and build Beijing into an ecological city surrounded by blue sky, clear water, and forests by 2035. We will fully tap the potential of energy conservation and carbon reduction in the adjustment of the industrial, energy, and functional structures, and build low-carbon cities with world-class standards.

In this context, we calculated and analyzed the spatiotemporal changes of energy carbon emissions and the vegetation carbon budget in Beijing from 2010 to 2020 to grasp the composition structure and influencing factors of carbon emissions and carbon sinks. On the basis of the 2006 IPCC Guidelines for National Greenhouse Gas Inventories and the Guidelines for the Preparation of Provincial Greenhouse Gas Emission Inventories, the energy emission accounting list and related parameters of Beijing were determined, the carbon emissions of the energy sector of Beijing in 2010 and 2020 were calculated, and the spatial distribution model of energy carbon flux was established. The carbon flux and spatial distribution of the vegetation ecosystem in Beijing in 2010 and 2020 were calculated using the C-FIX model. The research content and results provide data support for Beijing's energy conservation and emission reduction, urban fine management, ecological security pattern planning, and territorial space planning, and help the high-quality development of the capital.

2. Research Methods and Data Sources

2.1 Study area

As a political center, cultural center, international exchange center, and scientific and technological innovation center, Beijing is one of China's famous historical and cultural cities and ancient capitals (Fig. 1). As of 2020, the permanent population of Beijing was 21.893 million (according to the seventh national population census report), the regional GDP was 3610.26 billion yuan (Beijing Statistical Yearbook), and the urban forest coverage rate was 44.4%. Compared with 2010, the population increased by 11.63%, the regional GDP increased by 141.26%, the per capita GDP increased by 117.12%, and the forest coverage rate increased by 7.4%.

In recent years, owing to the rapid development of the city, the climate warming speed has increased and the average temperature in Beijing increased from 12.6 °C in 2010 to 13.8 °C in 2020 (an increase of 1.2 °C in ten years). To restore the urban ecological environment and slow down climate warming, Beijing had put forward the strategic goals of increasing the green area, improving the forest coverage rate, and reducing carbon emissions.

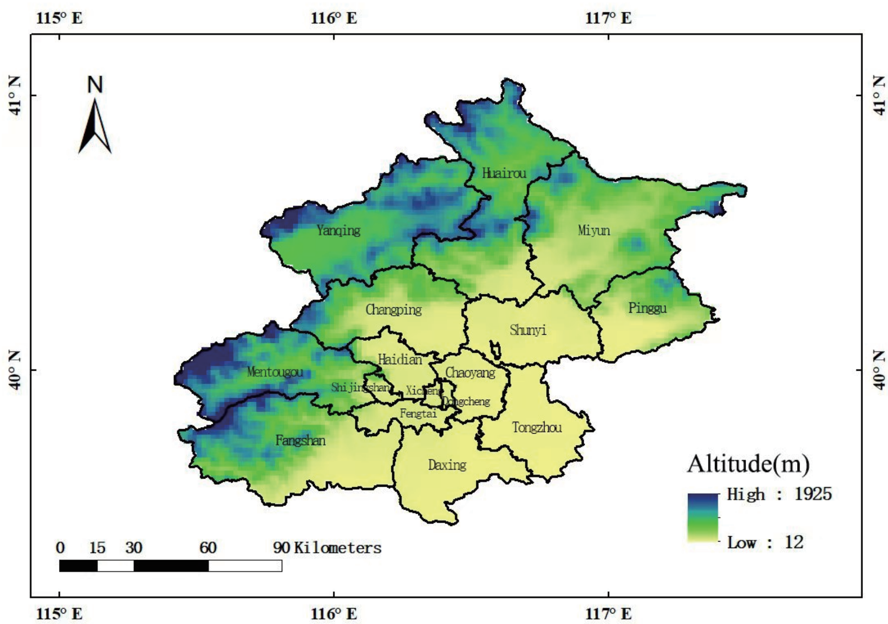

Fig. 1. (Color online) Elevation of Beijing.

2.2 Research method

2.2.1 C-FIX model

Terrestrial ecosystems absorb CO_2 from the atmosphere and convert it into organic matter, which has a positive effect on reducing carbon dioxide emissions and is of great significance for the realization of the national "two-carbon" strategy. Net Ecosystem Productivity (NEP) is the difference between net primary productivity (NPP) and soil heterotrophic respiration (Rh), which is the net carbon storage capacity of a terrestrial ecosystem and quantitatively describes the carbon source/sink capacity of the terrestrial ecosystem. NEP > 0 means that the ecosystem acts as a carbon sink and the opposite means that it is a carbon source. Therefore, NEP reflects the material circulation and energy flow of the ecosystem, and is an important indicator of carbon sinks.[14–16]

The C-FIX model is a light energy utilization model based on Montes Theory[17] and is capable of simulating the three basic carbon cycle components estimated at regional and global scales [total primary productivity (GPP), NPP, and NEP]. In recent years, many scholars have used the C-FIX model to simulate GPP, NPP, and NEP, and obtained good simulation results.[20–22] For each pixel, GPP, NPP, and NEP are estimated daily using Eqs. (1) to (8). Tables 1 through 3 list the parameters of the C-Fix model.[17]

$$GPP_d = p\left(T_{atm}\right) \times CO_2 fert \times \varepsilon \times fAPAR \times c \times S_{g,d} \tag{1}$$

$$NPP_d = GPP_d \times \left(1 - A_d\right) \tag{2}$$

$$NEP_d = NPP_d - R_{h,d} \tag{3}$$

$$p\left(T_{atm}\right) = \frac{e^{\left(C_1 \frac{\Delta H_{a,p}}{R_g \cdot T}\right)}}{1 + e^{\left(\frac{\Delta S \cdot T - \Delta H_{d,p}}{R_g \cdot T}\right)}} \tag{4}$$

$$CO_2 fert = \frac{\left[CO_2\right] - \frac{\left[O_2\right]}{2\tau} K_m \left(1 + \frac{\left[O_2\right]}{K_0}\right) + \left[CO_2\right]^{ref}}{\left[CO_2\right]^{ref} - \frac{\left[O_2\right]}{2\tau} K_m \left(1 + \frac{\left[O_2\right]}{K_0}\right) + \left[CO_2\right]} \tag{5}$$

$$fAPAR = 1.1638 \times NDVI - 0.1426 \tag{6}$$

$$A_d = \left(7.825 + 1.145 T_a\right) / 100 \tag{7}$$

Table 1
Parameters of the C-FIX model.

Parameter	Significance	Value	Unit
$p(T_{atm})$	Normalized temperature dependence factor[18] [0,1]		[-]
CO_2fert	Normalized CO_2 fertilization factor[17]		[-]
ε	Radiation use efficiency (RUE)		gC/MJ
C	Climatic efficiency[19]	0.48	[-]
$S_{g,d}$	Incoming daily global radiation		MJ/m^2/d
A_d	Autotrophic respiratory fraction[24]		[-]
$R_{h,d}$	Heterotrophic respiration[25]		gC/m^2/d
$fAPAR$	Fraction of absorbed photosynthetically active radiation (PAR)[26]		

ε in Eq. (1) was assigned in accordance with the different land use types in Table 2.

Table 2
Radiation use efficiency (e) of vegetation for different land use types.[23]

Land use types	$\mathcal{E}$ (gC/MJ)	Land use types	$\mathcal{E}$ (gC/MJ)
Evergreen coniferous forest	1.01	Shrubland	0.83
Evergreen broad-leaved forest	1.26	Grassland	0.61
Deciduous coniferous forest	1.10	Agriculture	0.60
Deciduous broad-leaved forest	1.04	Savanna	0.77
Mixed forest	1.12	Sparse vegetation	0.39
		Others	0.39

Table 3
Parameters used in Eqs. (4)–(8).[13]

Parameter	Significance	Value	Unit
C_1	Constant	21.77	
$\Delta H_{a,p}$	Activation energy	52750	J/mol
ΔS	Entropy of denaturation equilibrium of CO_2	704.98	J/K/mol
R_g	Gas constant	8.31	J/K/mol
T	Air temperature		K
T_a	Air temperature		°C
$\Delta H_{d,p}$	Deactivation energy	211000	J/mol
τ	CO_2/O_2 specificity ratio		
$[CO_2]$	CO_2 concentration in mesophyll tissue of leaves		ppmv
$[O_2]$	O_2 concentration in mesophyll tissue of leaves	20.9	ppmv
$[CO_2]^{ref}$	CO_2 concentration in atmosphere	285	ppmv
K_m	Affinity constant for CO_2 of Rubisco		[%CO_2]
K_0	Inhibition constant for O_2		[%O_2]
$NDVI$	Normalized difference vegetation index		
$k_{s,y}$	Heterotrophic respiratory rate coefficient		gC/m^2/d
Q_{10}	Relative increase in respiratory flux for 10 K increase in temperature T_a	1.5	

$$R_{h,d} = k_{s,y} \cdot Q_{10}^{T_a/10} \tag{8}$$

The affinity coefficients K_m and K_0 show a temperature dependence that follows an Arrhenius relationship:

$$K_m = Ae^{\left(-E_a/R_gT\right)}. \tag{9}$$

If $T_a \geq 15$ °C, $E_a = 59.4$ kJ/mol and $A = 2.419 \times 1013$, or if $T_a < 15$ °C, $E_a = 109.6$ kJ/mol and $A = 1.976 \times 1022$.

The inhibition constant K_0 for O_2 is calculated using Eq. (10), where $A_0 = 8240$ and $E_{a0} = 13.9135$ kJ/mol.

$$\tau = A_\tau e^{\left(-E_{a\tau}/R_gT\right)} \tag{10}$$

Here, $A_\tau = 7.87 \times 10^{-5}$ and $E_a = -42.8969$ kJ/mol.

$$k_{s,y} = \frac{\sum_{d=1}^{365} \frac{GPP_d}{b_y}}{\sum_{d=1}^{365} p\left(T_{atm}\right)_d} \tag{11}$$

The parameter b_y is the mean annual calibration coefficient of soil heterotrophic respiration, and its value is 1.0.

2.2.2 Energy carbon emission accounting

On the basis of the above determination of the carbon emission range of energy consumption in human activities, we adopted the top-down international energy consumption carbon emission accounting method, referring to the carbon emission accounting list in the 2006 IPCC National Greenhouse Gas Inventory Guide and the Provincial Greenhouse Gas Inventory Preparation Guide prepared by China. The accounting model is

$$E = \sum_j C_j \times I_j = \sum_j C_j \times L_j \times P_j \times O_j \times \frac{44}{22}, \tag{12}$$

where E is the total carbon emission generated by human-induced energy consumption, j is the energy type, C is the physical amount of energy consumption, I is the carbon emission factor, L is the low calorific value of energy, P is the carbon content per unit calorific value of energy (kJ/m^3 or kJ/kg), and O is the oxidation rate (%) in the process of energy combustion. 44/12 is the conversion coefficient of carbon to carbon dioxide.

The IPCC guidelines provide emission factors for carbon emission accounting for various energy sources. Since there are some differences in energy type and energy quality among countries around the world, the IPCC guidelines recommend using specific values to account for carbon emissions in accordance with the country and region, so as to accurately reflect the trend of carbon emissions of different energy qualities and countries and reduce uncertainty. In this context, China compiled the Guidelines for the Compilation of Provincial GHG Inventories in line with China's national conditions, providing a valuable reference for China's carbon emission accounting. Using carbon content and oxidation rate in the guidelines in combination with the General Principles for the Calculation of Comprehensive Energy Consumption, we obtained parameters that can be used to calculate carbon emissions from various energy sources in China (Table 4). There are many types of energy with different amounts of heat contained. To facilitate mutual comparison and research on the total amount, China stipulated the calorific value of standard coal to be 7000 kcal/kg (29.3076 GJ/t). The carbon content of coking coal was 25.86 kg/GJ, and the CO_2 emission coefficient of standard coal was 2.7725 tCO_2/tce.

2.2.3 Spatial distribution methods of energy carbon emissions

The purpose of spatial allocation was to grid energy carbon emissions at the administrative level, that is, by selecting certain parameters (such as population and GDP), the emissions per administrative unit were processed into emissions per grid unit. In this study, the precision of the urban scale simulation grid depended on the spatial precision of the parameters, and the resolution was 1 × 1 km.

The space allocation methods commonly used were the spatial interpolation and weight methods. In this study, the weight method was mainly used. The specific steps were as follows.

The first step was to extract 1 km grid maps of GDP and population in different administrative regions of Beijing referring to the existing administrative boundary map at the city level and using the segmentation function of ArcGIS, as the spatial allocation base map for GDP and population.

The second step was to calculate the grid emission coefficient of GDP and population parameters of each of 16 administrative districts of Beijing. The specific formula was

Table 4
Carbon emission accounting parameters of various energy sources.

Energy type	Low calorific value (GJ/KJ; GJ/10^4 m^3)	Carbon content per unit calorific value (tC/GJ)	Carbon oxidation rate (%)	Conversion coefficient of standard coal (kgce/kg)
Raw coal	20.908	0.02637	94	0.7143
Cleaned coal	26.344	0.0274	94	0.9
Coal products	19.25	0.03	92	0.72
Coke	28.435	0.0295	93	0.9714
Natural gas	38.931	0.0153	99	1.21
Steam oil	43.07	0.0189	98	1.4714
Coal oil	43.07	0.0196	98	1.4714
Diesel oil	42.652	0.0202	98	1.4571
Fuel oil	41.816	0.0211	98	1.4286
Liquefied petroleum gas	50.179	0.0172	99	1.7143
Refinery dry gas	45.998	0.0182	98	1.5714
Heat				0.03412
Electricity				0.1229
Standard coal	29.3076	0.02586	94	

$$A_{ij} = \frac{D_{ij}}{\sum_{i=1}^{n} D_{ij}}, \tag{13}$$

where A_{ij} is the carbon emission coefficient of pixel i in region j and D_{ij} is the carbon emission intensity of pixel i in region j. The energy carbon emissions of the primary, secondary, and tertiary industries were calculated using GDP, and the carbon emissions of residential energy were calculated using population.

The third step was to assign the carbon emission values in administrative districts to the grid. The specific formula was

$$E_{ij} = A_{ij} \times C_j, \tag{14}$$

where E_{ij} is the energy carbon emission of an industry type in pixel i of zone j, A_{ij} is the carbon emission coefficient of an industry type in pixel i of zone j, and C_j is the total energy carbon emission of an industry type in zone j.

2.3 Data source

2.3.1 Land-use-type data

Cities are the main sources of carbon emissions due to their high level of industrialization and dense population. As a megacity, Beijing's carbon budget has attracted much attention from the state and scholars. In the Master Plan of Beijing City (2016–2035), it was proposed that by 2020, Beijing's environmental quality would be generally improved, the level of a green, low-carbon lifestyle would be further improved, and the development goal of building Beijing into an ecological city with blue sky, clear water, and forests by 2035 would be attained. It is necessary to properly handle the internal links between urban development and the utilization of resources and energy, the improvement of environmental quality, and the joint response to climate change, and to promote the green, low-carbon transformation of the economy and society. We should fully tap the potential of energy conservation and carbon reduction in the adjustment of industrial, energy, and functional structures, and build low-carbon cities with world-class standards. We should also enhance the adaptive capacity of urban infrastructure and the carbon sequestration capacity of urban systems, enhance the emergency response capacity to extreme climate events, and build Beijing into a climate-smart demonstration city.

In this study, using the vector map of Beijing's administrative boundaries, the land use types of Beijing in 2010 and 2020 were extracted with a resolution of 30 m. The soil data came from the GlobeLand30 land use product released by China. The product, developed by China, provided the global land cover data with a 30 m spatial resolution. The GlobeLand30 2000 and 2010 editions were released in 2014. GlobeLand30 data included 11 primary land use types, namely, cultivated land, forest land, grassland, shrub land, wetland, water body, tundra, artificial surface, bare land, glacier, and permanent snow.

2.3.2 NPP data

NPP was obtained using EARTHDATA's MOD17A3HGF V6 product, which provides annual NPP information at a 500 m pixel resolution. The temporal resolution was year by year, the spatial resolution was 500 m in kg carbon/m^2/year (kgC/m^2/year), and the geographical coordinate system was WGS 1984.

2.3.3 Socioeconomic data

The socioeconomic data were collected from the Resources and Environmental Science and Data Center of the Institute of Geographic Sciences and Natural Resources Research, Chinese Academy of Sciences. The socioeconomic grid data designed in this study included two types of data: population data and GDP data.

We downloaded the 2010 and 2019 China population and GDP spatial distribution dataset with a 1 km grid. The dataset reflected the detailed spatial distribution of the population and GDP across the country. The data were in a grid format and were based on the Krassovsky ellipsoid. The projection method used was Albers projection.

2.3.4 Statistical data

Statistics mainly included population, GDP, and energy consumption, among others. The GDP and energy consumption data were from the 2011 and 2021 statistical yearbooks of Beijing administrative districts. The population data were obtained from the Sixth and Seventh Census Bulletins of Beijing Municipality.

3. Results and Analysis

3.1 Energy carbon emission in Beijing

In 2020 (compared with 2010), the total carbon emission from energy consumption in Beijing was reduced by 36.78%, and the total carbon emission from energy consumption in most administrative regions was reduced by varying degrees. In terms of spatial distribution, by 2020, the total carbon emission from energy consumption in Beijing (compared with 2010) had gradually decreased from outside to inside of the city. Among all districts, the reduction ratio of energy carbon emissions in an ecological conservation area was generally higher than that in urban Districts of 6 (Table 5, Fig. 2). The energy carbon emissions of Dongcheng and Fengtai administrative districts had increased, while those of the other regions had decreased. Among them, Changping, Daxing, and Tongzhou showed significant reductions. Secondly, the spatial distribution of total carbon emissions from energy consumption and land use cover-type data was consistent.

The carbon emissions of energy consumption in the secondary industry of each administrative region decreased significantly. Among them, the carbon emissions of industrial energy

Table 5
Total carbon emissions from energy consumption. (Unit: 10^4 tCO_2)

Administrative region	2010	2020	Rate of change	Administrative region	2010	2020	Rate of change
Dongcheng	773.06	838.60	8.48	Tongzhou	765.38	82.96	−89.16
Xicheng	1141.99	994.22	−12.94	Shunyi	2356.57	–	–
Chaoyang	2746.47	2405.09	−12.43	Changping	881.37	44.23	−94.98
Fengtai	1061.95	1247.83	17.50	Daxing	671.22	83.34	−87.58
Shijingshan	1792.84	331.65	−81.50	Huairou	276.72	31.07	−88.77
Haidian	2091.77	1964.93	−6.06	Pinggu	266.19	28.41	−89.33
Mentougou	198.32	158.39	−20.13	Miyun	259.09	32.34	−88.58
Fangshan	2405.97	-	-	Yanqing	137.10	15.86	−88.43

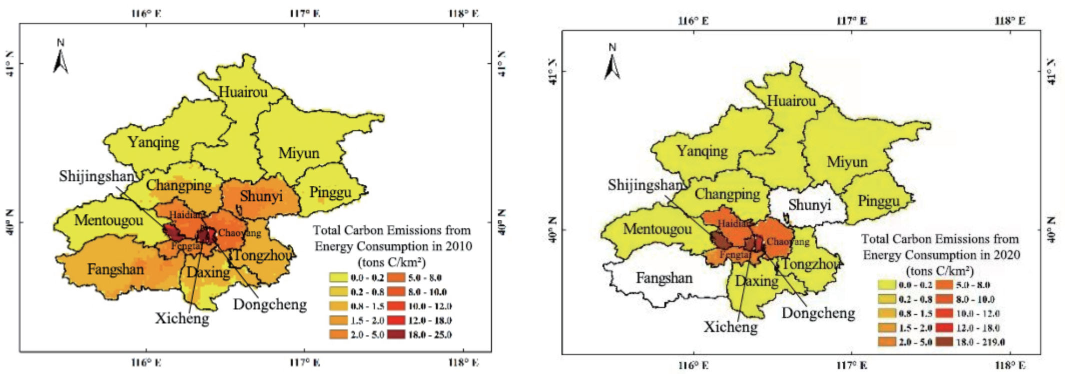

(a) (b)

Fig. 2. (Color online) Total carbon emissions from energy consumption in each administrative region of Beijing.

particularly decreased. The analysis showed that the proportion of industrial carbon emissions in secondary industry energy carbon emissions was much higher than that of the other industries such as construction (Table 6, Fig. 3). By 2020, this proportion decreased, and the proportion of industrial carbon emissions in each administrative region was mainly distributed between 69.76 and 91.28%. According to the statistics, the carbon emissions of industrial energy in each administrative region decreased significantly, except for Xicheng and Fengtai, where they increased slightly. Compared with 2010, industrial carbon emissions in each administrative region decreased by more than 65.58% by 2020. Among them, the industrial carbon emissions in Shijingshan, Huairou, and Daxing decreased by 96.49, 92.86, and 92.76%, respectively.

We found that the demand for energy in residential life has increased significantly over the past decade. The overall decrease in household carbon emissions was mainly due to the decrease in household carbon emissions in Tongzhou, Daxing, Huairou, Yanqing, and the other regions (Fig. 3). According to the statistics, by 2020 (compared with 2010), the carbon emissions of residents had been reduced by 77.52%. The living carbon emissions of Dongcheng, Xicheng, Chaoyang, Fengtai, Mentougou, and the other districts showed an increasing trend, while the living carbon emissions of residents in Tongzhou, Daxing, Huairou, Yanqing, and the other areas decreased. The areas where the carbon emissions of residents increased were mainly concentrated in places with large populations and more frequent human activities.

Table 6
Secondary industry energy carbon emissions and changes. (Unit: 10^4 tCO_2)

Administrative region	Secondary industry			Industry		
	2010	2020	Variation quantity	2010	2020	Variation quantity
Dongcheng	56.84	24.68	−32.16	–	–	–
Xicheng	136.68	139.15	2.47	116.72	122.93	6.21
Chaoyang	761.69	289.28	−472.41	704.77	242.57	−462.20
Fengtai	187.98	217.00	29.03	151.54	159.55	8.01
Shijingshan	1600.87	68.90	−1531.97	1577.66	55.39	−1522.27
Haidian	425.80	–	−425.80	–	–	–
Mentougou	87.17	23.29	−63.88	80.79	16.25	-−64.54
Fangshan	–	–	–	–	–	–
Tongzhou	289.23	15.15	−274.08	–	9.45	–
Shunyi	–	–	–	–	–	–
Changping	219.37	32.92	−186.45	–	–	–
Daxing	205.72	14.94	−190.78	184.93	13.39	−171.53
Huairou	142.67	10.27	−132.41	131.17	9.37	−121.80
Pinggu	–	6.17	–	–	–	–
Miyun	–	8.25	–	–	6.72	–
Yanqing	31.63	2.28	−29.35	–	–	–

Note:“-”indicates data not available in the statistical yearbook.

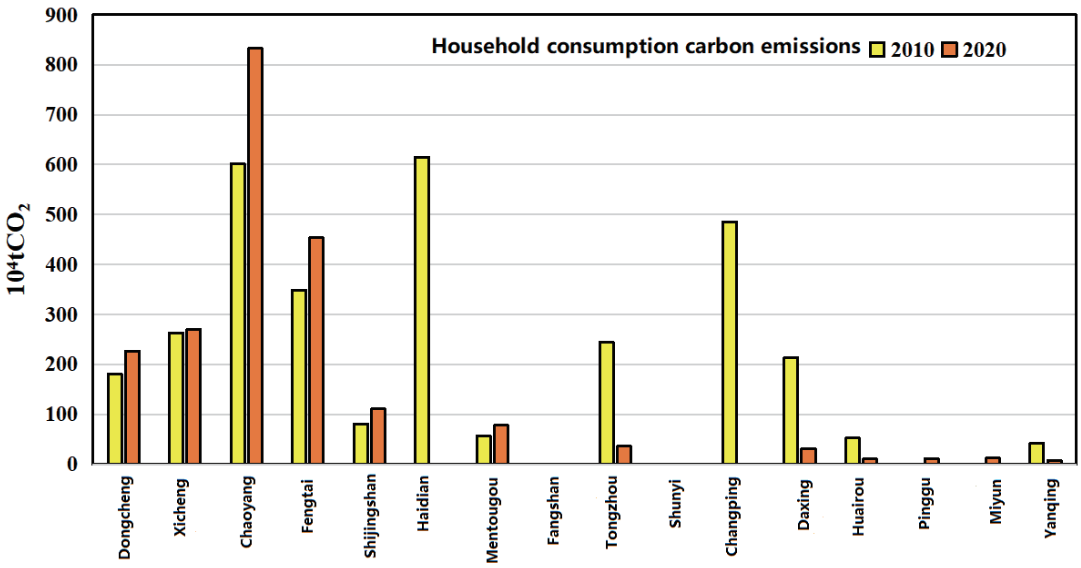

Fig. 3. (Color online) Carbon emissions from household consumption.

According to the sixth and seventh censuses of Beijing, the permanent populations of Dongcheng, Xicheng, Chaoyang, and Fengtai decreased by about 22.87, 11.02, 2.6, and 4.4%, respectively, between 2010 and 2020. Most of the carbon emissions in residential life came from electricity, heating, gas, and family cars. In the case of population reduction, the energy carbon emissions generated by residents still increased, which indicated that the demand for energy in residents’ lives had risen significantly in the past decade.

3.2 Analysis of vegetation carbon budget in Beijing

The vegetation areas of the whole city showed a carbon sink function, and most of the administrative regions had enhanced carbon sink capacity. The total carbon flux of vegetation in Beijing was determined to be 1647.68 × 10^4 tCO_2 in 2010 and 2097.94 × 10^4 tCO_2 in 2020. Compared with that in 2010, the total vegetation carbon flux in 2020 increased by 27.33% (450.26 × 10^4 tCO_2). According to statistics, the carbon sink capacities of vegetation in Shijingshan, Haidian, and Miyun decreased by 1.38 × 10^4, 3.87 × 10^4, and 8.69 × 10^4 tCO_2 in 2020, respectively.

Regions of vegetation in Dongcheng, Xicheng, Chaoyang, Fengtai, Shijingshan, Tongzhou, and Daxing were carbon sources, and the other regions were carbon sinks. In 2010 and 2020, the total carbon flux of vegetation in Dongcheng, Xicheng, Chaoyang, Fengtai, Shijingshan, Tongzhou, and Daxing was negative, so they were carbon sources. Shijingshan was a carbon sink in 2010 but had converted to a carbon source by 2020, whereas Shunyi had converted from a carbon source in 2010 to a carbon sink by 2020. Compared with 2010, vegetation carbon fluxes in Dongcheng, Shijingshan, and Daxing regions decreased by 2020, while the total vegetation carbon fluxes in the other administrative regions showed varying degrees of increase in the range from 0.01 to 80 × 10^4 tCO_2 (Table 7). The carbon fluxes of cultivated land, forest land, grassland, and shrub in each administrative region were analyzed.

Most of the cultivated land in the administrative region acted as carbon sinks, but the carbon sink capacity decreased. In 2020, except for Xicheng where there was no cultivated land, the cultivated land in most areas showed the carbon sink function, among which the cultivated land in Shijingshan and Shunyi had changed from being carbon sources in 2010 to carbon sinks by 2020. However, note that half of the administrative regions showed varying degrees of decrease

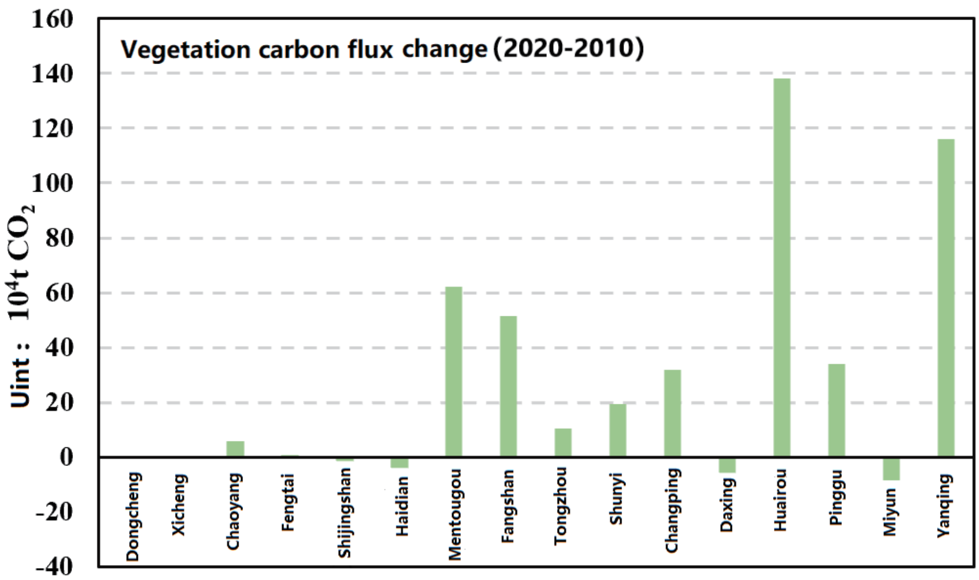

Fig. 4. (Color online) Changes in vegetation carbon flux in each administrative region.

Table 7
Vegetation carbon flux and its change in each administrative region. (Unit: 10^4 tCO_2)

Administrative region	2010	2020	Variation quantity	Administrative region	2010	2020	Variation quantity
Dongcheng	−0.23	−0.23	−0.01	Tongzhou	−23.94	−13.60	10.34
Xicheng	−0.11	−0.11	0.01	Shunyi	−3.48	16.00	19.48
Chaoyang	−8.84	−3.04	5.80	Changping	130.05	161.75	31.70
Fengtai	−6.85	−5.92	0.93	Daxing	−33.42	−39.16	−5.74
Shijingshan	0.10	−1.28	−1.38	Huairou	421.19	559.23	138.04
Haidian	9.32	5.45	−3.87	Pinggu	116.58	150.47	33.90
Mentougou	227.99	290.18	62.20	Miyun	294.87	286.18	−8.69
Fangshan	221.69	273.29	51.60	Yanqing	302.78	418.72	115.94

in cultivated land carbon flux in 2020 (Fig. 5), mainly due to the reduction in cultivated land area.

In Shijingshan, Daxing, Pinggu, and Yanqing, the total carbon flux of cultivated land still increased while the cultivated land area decreased. Among them, Shijingshan and Daxing were carbon sources, and their carbon source capacity increased. Pinggu and Yanqing showed the function of a carbon sink, and their carbon sink capacity increased.

The forest land in the whole city showed the function of a carbon sink, and the carbon sink capacity increased. In 2010 and 2020, the total carbon flux of forest land was determined to be 1287.33×10^4 and 1710.02×10^4 tCO_2, respectively. By 2020, the whole forest land showed a carbon sink function and the carbon sink capacity had increased by 422.69×10^4 tCO_2. The carbon sink of forest land mainly reflected the regions with large forest land areas, and the carbon source function was manifested in the regions with less forest land (Table 8).

The forest land in the central area of the city was a carbon source, and the suburban area was a carbon sink; the carbon flux of forest land in most areas showed an increasing trend. The analysis results showed that in areas with more forest land distribution (such as Mentougou, Fangshan, Changping, Huairou, Pinggu, Miyun, and Yanqing), forest land showed the carbon sink function, although the carbon sink capacity increased by different degrees (Fig. 6 and Table 8). The carbon sink capacity of Huairou increased the most, 125.08×10^4 tCO_2, followed by those of Yanqing, Mentougou, and Fangshan, with increases of 96.62×10^4, 71.81×10^4, and 63.97×10^4 tCO_2, respectively. Dongcheng, Xicheng, Chaoyang, Fengtai, Shijingshan, Tongzhou, and Daxing showed the function of a carbon source, except that the carbon source capacities of Shijingshan, Tongzhou, and Daxing continued to increase, whereas those of the other regions decreased. This was mainly due to the reduction in forest area in the above regions. In addition, although Haidian had always shown a carbon sink function, its carbon sink capacity decreased by 0.91×10^4 tCO_2.

The average carbon flux of forest land increased in most areas, and the quality of forest land was generally good. The average carbon flux of forest land in Fengtai, Shijingshan, Haidian, and Daxing areas showed a downward trend, decreasing by 51.88, 106.00, 34.44, and 28.12 g C/m^2/year, respectively. The average carbon flux of forest land in the other areas increased to different degrees, indicating that the quality of forest land in the city was generally good. According to

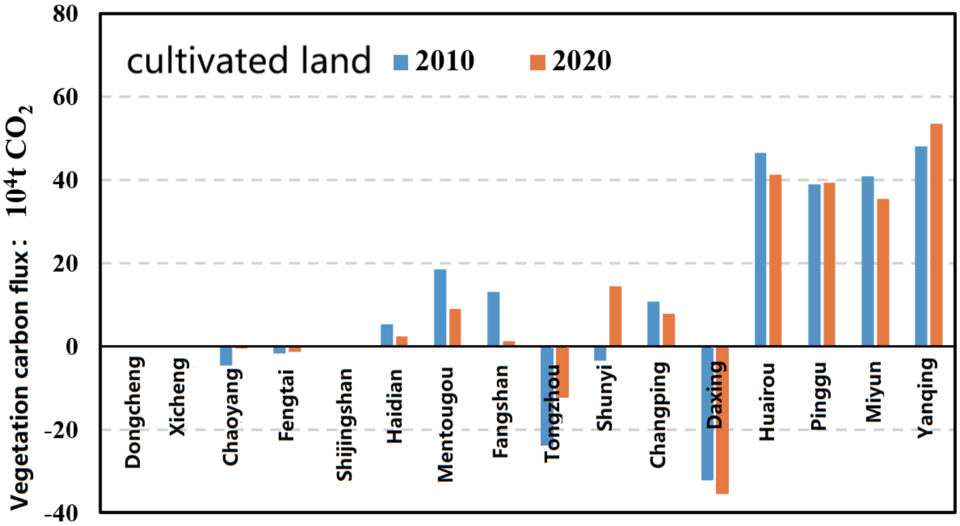

Fig. 5. (Color online) Carbon flux of cultivated land in each administrative region.

Table 8
Carbon flux and change of forest land in each administrative region. (Unit: 10^4 tCO_2)

Administrative region	2010	2020	Variation quantity	Administrative region	2010	2020	Variation quantity
Dongcheng	−0.23	−0.23	0.00	Tongzhou	−0.08	−0.16	−0.08
Xicheng	−0.11	−0.10	0.01	Shunyi	−0.14	1.61	1.75
Chaoyang	−4.08	−1.61	2.48	Changping	102.87	136.16	33.29
Fengtai	−4.73	−3.45	1.28	Daxing	−0.44	−0.62	−0.19
Shijingshan	−0.36	−0.96	−0.60	Huairou	324.75	449.83	125.08
Haidian	2.17	1.26	−0.91	Pinggu	60.99	86.91	25.92
Mentougou	192.50	264.31	71.81	Miyun	198.46	200.72	2.26
Fangshan	199.11	263.08	63.97	Yanqing	216.64	313.26	96.62

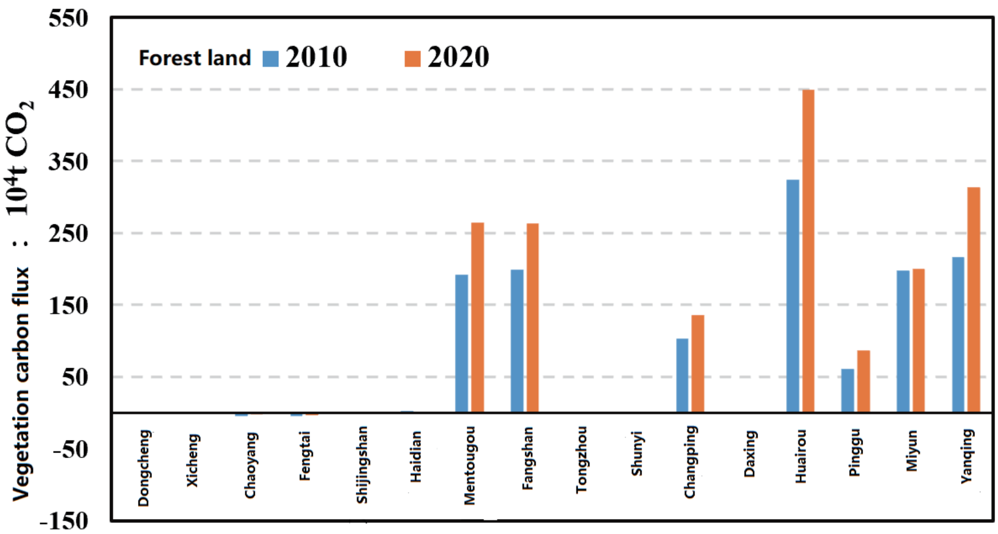

Fig. 6. (Color online) Carbon flux of forest land in each administrative region.

the data of land cover type, the woodland area of Fengtai, Shijingshan, and Haidian had decreased by 2020 (compared with 2010), and the woodland area of Fengtai and Shijingshan had decreased by 11 and 7.58%, respectively (Fig. 7). Although the forest area of Xicheng and Chaoyang also decreased correspondingly, the average carbon flux increased because the forest area decreased less and the forest trees were relatively young. Although the area of forest land increased slightly in Daxing, the average carbon flux of forest land decreased, indicating that the quality of forest land was poor, which might be caused by the older forest age.

Grassland in the whole city showed the carbon sink function, and the carbon sink capacity of grassland in Huairou, Pinggu, and Yanqing increased significantly. In 2010 and 2020, the total carbon flux of grassland in the city was 204.19×10^4 and 233.40×10^4 tCO_2, and the carbon flux increased by 29.21×10^4 tCO_2. The analysis showed that the increase in grassland carbon flux in the whole city was mainly due to the increase in grassland carbon flux in Huairou, Pinggu, and Yanqing (Fig. 8). The grassland area of Yanqing among the above three regions decreased slightly (−0.56%), while those of Huairou and Pinggu remained relatively stable, increasing by 0.05 and 0.38%, respectively. At the same time, the average carbon flux in the three regions also showed a significant upward trend (Fig. 8). Therefore, the grassland quality in Huairou, Pinggu, and Yanqing was higher than that in the other districts.

Most grassland in urban areas acts as a carbon source, and most grassland in suburban areas acts as a carbon sink, the capacity of which was reduced in most areas, and the quality of grassland was poor. The analysis results showed that in 2020, except for Haidian, Mentougou, Shunyi, Changping, Huairou, Pinggu, Yanqing, and Miyun, all other regions acted as carbon sinks. At the same time, the grassland carbon sink capacity increased in Haidian, Changping, Huairou, Pinggu, and Yanqing, while the grassland carbon flux decreased to different degrees in the other areas (Fig. 8). Compared with the changes in grassland area in different districts, the

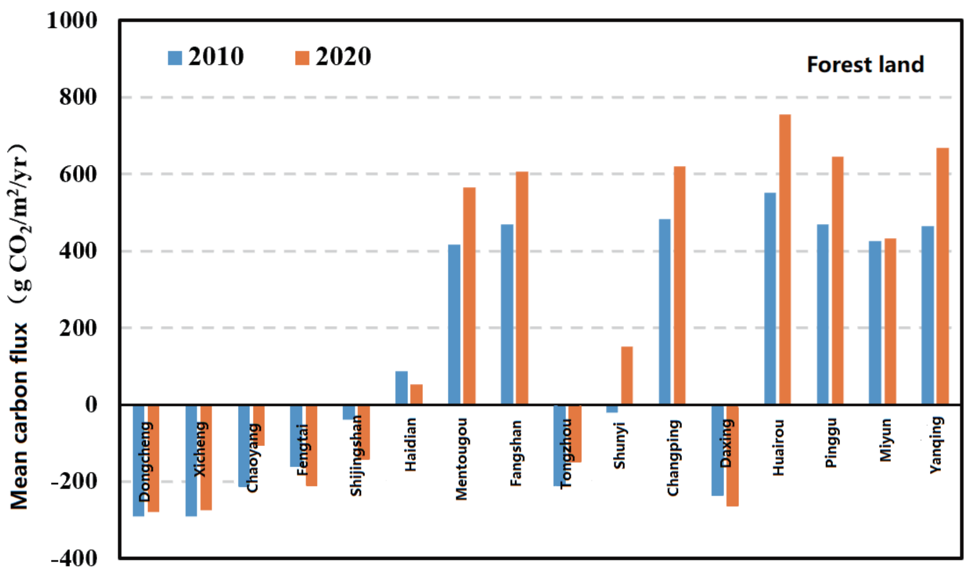

Fig. 7. (Color online) Average carbon flux of forest land in each administrative region.

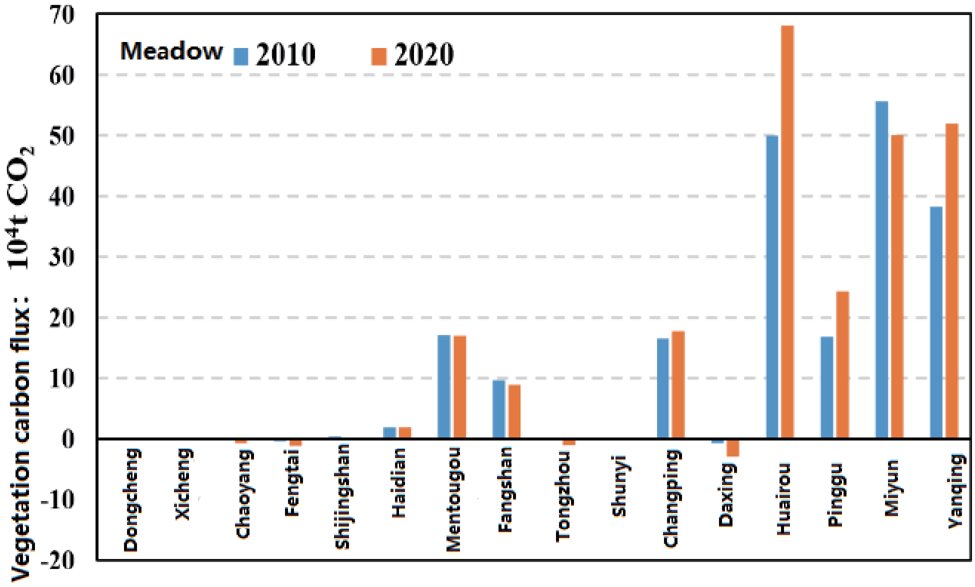

(a)

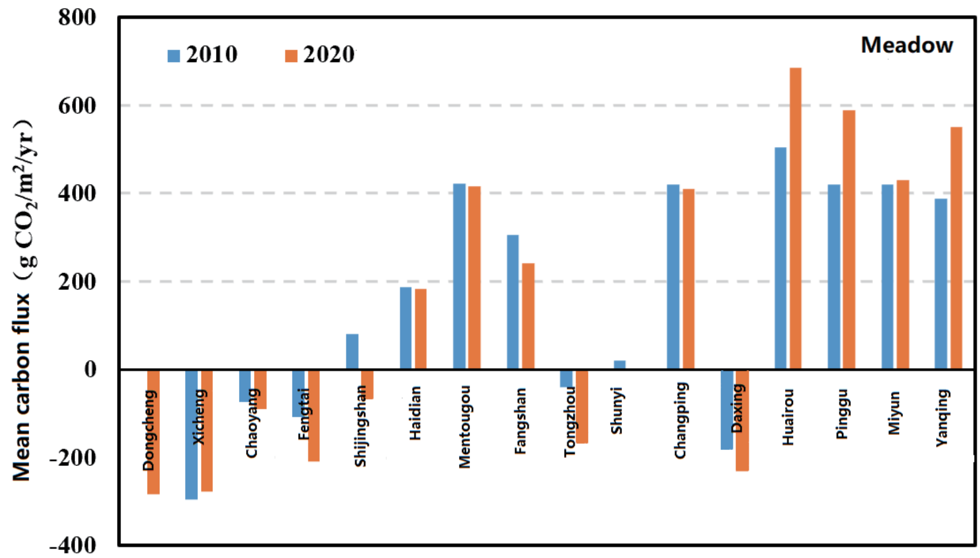

(b)

Fig. 8. (Color online) Carbon flux and average carbon flux of grassland in each administrative region.

grassland areas in Shijingshan, Miyun, and Yanqing decreased in 2020, while those in the other areas increased to different degrees. Combined with the above results, it could be concluded that the areas where the grassland carbon sink capacity decreased or the grassland was a carbon source were mainly a result of poor grassland quality.

3.3 Comparison of vegetation carbon sequestration and energy carbon emissions

Vegetation carbon uptake was lower than energy carbon emissions, but the gap was greatly reduced, as shown by a comparison between energy carbon emissions and vegetation carbon flux (Table 9). In 2010, the total energy carbon emission of Beijing was 17826 × 10^4 tCO_2, and the carbon absorption by vegetation was 1647.68 × 10^4 tCO_2. In 2020, the total energy carbon emission of Beijing was 8258.92 × 10^4 tCO_2, and the carbon absorption by vegetation was 2097.94 × 10^4 tCO_2. Although the carbon sink capacity of vegetation was much lower than the carbon emissions from energy in the past decade, the gap was greatly reduced.

Areas with high vegetation cover made an important contribution to carbon uptake. In 2020, the vegetation in Mentougou, Fangshan, Changping, Huairou, Pinggu, Miyun, and Yanqing regions showed increased carbon sink function and carbon sink capacity, and the vegetation coverage in these regions was higher.

4. Conclusions and Discussion

We established a spatial model of energy carbon emissions in Beijing in 2010 and 2020 and calculated and analyzed the spatiotemporal changes in energy carbon emissions and the vegetation carbon budget in Beijing in the past 10 years and the influencing factors. The main conclusions were as follows.

1) Vegetation carbon uptake in Beijing was lower than energy carbon emissions, but the gap was greatly reduced. Compared with 2010, the carbon emissions from energy consumption in

Table 9
Energy carbon emission and vegetation carbon flux in Beijing. (Unit: 10^4 tCO_2)

	2010		2020	
	Carbon emission	Carbon sequestration by vegetation	Carbon emission	Carbon sequestration by vegetation
Dongcheng	773.06	−0.23	838.60	−0.23
Xicheng	1141.99	−0.11	994.22	−0.11
Chaoyang	2746.47	−8.84	2405.09	−3.04
Fengtai	1061.95	−6.85	1247.83	−5.92
Shijingshan	1792.84	0.10	331.65	−1.28
Haidian	2091.77	9.32	1964.93	5.45
Mentougou	198.32	227.99	158.39	290.18
Fangshan	2405.97	221.69	–	273.29
Tongzhou	765.38	−23.94	82.96	−13.60
Shunyi	2356.57	−3.48	–	16.00
Changping	881.37	130.05	44.23	161.75
Daxing	671.22	−33.42	83.34	−39.16
Huairou	276.72	421.19	31.07	559.23
Pinggu	266.19	116.58	28.41	150.47
Miyun	259.09	294.87	32.34	286.18
Yanqing	137.10	302.78	15.86	418.72
Total	17826.01	1647.68	8258.92	2097.94

Beijing had decreased by 36.78% and the total carbon flux from vegetation had increased by 27.33% in 2020. On the whole, China's policies on energy conservation, emission reduction, and ecological protection have achieved remarkable results.

2) The total population of Dongcheng, Xicheng, Chaoyang, Fengtai, Mentougou, and the other districts showed a decreasing trend, but the domestic carbon emission showed an increasing trend. In the past ten years, the demand for energy in residents' lives increased significantly, and carbon emissions from the tertiary industry and residents' living energy became one of the important sources of carbon emissions in cities.

3) The vegetation areas of the whole city showed a carbon sink function, and most of the administrative regions had enhanced carbon sink capacity. The quality of forest land in the whole city was generally good, and the average carbon flux of forest land in most areas showed an increasing trend. However, grassland in urban areas mostly functions as a carbon source. Although suburban grassland showed a carbon sink function, the carbon sink capacity was reduced and the grassland quality was poor.

On the basis of the above conclusions, it is recommended to further reduce energy carbon emissions while enhancing the vegetation carbon sequestration capacity. To effectively reduce carbon emission levels, we suggest the formulation and implementation of energy-saving and emission reduction plans for the tertiary industry and domestic energy, and the proposal of supporting policies. The carbon emissions from the tertiary industry and residential energy have become one of the important sources of carbon emissions in cities. Therefore, it is necessary to sort out the industries and consumption structures involved in the tertiary industry and residential energy consumption. Combining carbon sequestration technology, we need to formulate and implement energy-saving and emission reduction plans for the tertiary industry and residential life, reduce carbon emissions by reducing energy consumption, reuse energy after increasing carbon emissions, and promote carbon sequestration technology. We propose energy-saving and emission reduction promotion policies, such as emission reduction targets, funding policies for the development and use of artificial carbon sequestration technologies, and preferential policies to provide assistance for the implementation of energy-saving and emission reduction plans.

In terms of increasing vegetation carbon sequestration, it is necessary to optimize grassland species types reasonably and enhance the grassland carbon sequestration capacity scientifically. Grassland, as one of the important vegetation types in Beijing, is of great significance in urban environmental planning and ecological security pattern construction. Therefore, to verify the distribution of grasslands in urban areas, it is necessary to sort out the types of grassland species in different regions, identify the causes of grassland carbon emissions, reasonably optimize the types of grassland planting species, improve grassland quality, and thereby enhance grassland carbon sequestration capacity.

Acknowledgments

Funding: Beijing Postdoctoral Research Foundation (2022-EE-096)

References

1 Summary for Policymakers. In Climate Change 2021: The Physical Science Basis. Contribution of Working Group I to the Sixth Assessment Report of the Intergovernmental Panel on Climate Change. Masson-Delmotte, V., P. Zhai, A. Pirani, S.L. Connors, C. Péan, S. Berger, N. Caud, Y. Chen, L. Goldfarb, M.I. Gomis, M. Huang, K. Leitzell, E. Lonnoy, J.B.R. Matthews, T.K. Maycock, T. Waterfield, O. Yelekçi, R. Yu, and B. Zhou Eds. (Cambridge University Press, Cambridge, United Kingdom and New York, NY, USA, 2021). https://doi.org/10.1017/9781009157896.001.

2 X. Fan, Y. Qin, X. Gao: Environ. Prot. **49** (2021) 44. https://doi.org/10.14026/j.cnki.0253-9705.2021.z2.008.

3 H. Akbari, S. Menon, and A. Rosenfeld: Climatic Change **94** (2003) 275. https://doi.org/10.1007/s10584-008-9515-9

4 K. George, L. H. Ziska, and J. A. Bunce: Environ. Sci. **41** (2007) 7654. https://doi.org/10.1016/J.ATMOSENV.2007.08.018

5 The Economics of Climate Change: The Stern Review, N. H. Stern Eds. (Cambridge University Press, 2007). https://doi.org/10.1017/CBO9780511817434

6 S. Tan, J. Yang, J. Y. Yan, C. Lee, H. Hashim, and B. Chen: Appl. Energy **185** (2017) 1919. https://doi.org/10.1016/j.apenergy.2016.03.041

7 Y. Li and Y.N. Li: Sustainable Cities Soc. **9** (2013) 62. https://doi.org/10.1016/j.scs.2013.03.001

8 D. Y. Liu, H. B. Du, F. Southworth, S. F. Ma: Transport. Res. Part A **105** (2017) 42. https://doi.org/10.1016/j.tra.2017.08.004

9 G. P. Peters, R. M. Andrew, T. Boden, J. G. Canadell, P. Ciais, C. L. Quéré, G. Marland, M. R. Raupach and C. Wilson: Nat. Clim Change **3** (2013) 4. https://doi.org/10.1038/nclimate1783

10 Y. Zhang, Z. Yang, and X. Yu: Environ. Sci. Technol. **49** (2015) 11247. https://doi.org/10.1021/acs.est.5b03060

11 L. Y. Shen, Y. Wu, C. Y. Shuai, W. S. Lu, K. W. Chau, and X. Chen: J. Cleaner Prod. **187** (2018) 348. https://doi.org/10.1016/j.jclepro.2018.03.190

12 L. Y. Shen, Y. Wu, L. Y. Lou, D. H. Zeng, C. Y. Shuai, and X. N. Song: J. Cleaner Prod. **174** (2018) 343. https://doi.org/10.1016/j.jclepro.2017.10.333

13 B. F. Cai, Y. Geng, W. S. Yang, P. Z. Yan, Q. L. Chen, D. Li, and L. B. Cao: J. Cleaner Prod. **149** (2017) 502. https://doi.org/10.1016/j.jclepro.2017.02.122

14 X. J. Chen, W. Zhou, and H. Yang: Arid Land Geogra. **43** (2020) 1583. URL

15 J. M. Chen, W. M. Ju, P. Ciais, N. Viovy, R. G. Liu, and X. H. Lu: Nat Commun. **4259** (2019). https://doi.org/10.1038/s41467-019-12257-8

16 Q. N. He, W. M. Ju, S. P. Dai, W. He, L. Song, S. H. Wang, X. C. Li, and G. X. Mao: JGR Biogeosci. **126** (2021). https://doi.org/10.1029/2020JG005944

17 F. Veroustraete: Ecol. Modell. **75** (1994) 221. https://doi.org/10.1016/0304-3800(94)90021-3

18 F. K. Y. Wang:Agric For Meteorol. **82** (1996) 1. https://doi.org/10.1016/0168-1923(96)02342-8.

19 K. J. McCree: Agric. Meteorol. **10** (1972) 442. https://doi.org/10.1016/0002-1571(72)90045-3.

20 D. Y. Zhang, Z. K. Feng, Y. Q. L. J. Li, Zhang, and B. Dong: Scientia Silvae Sinicae **47** (2011) 13. https://doi.org/10.1007/s11676-011-0141-4

21 H. M. Yan, J. Y. Zhan, F. Wu, H. C. Yang, and M. E. Chen: Energies **9** (2016) 260. https://doi.org/10.3390/en9040260

22 Lu, X. Li, and F. Veroustraete: Acta Ecologica Sinica **25** (2005) 1027. URL

23 L. J. Zhang, B. Y. Zhang, W. L. Li, X. X. Li, S. Li, and Q. Jiang: Ecol. Indic. **90** (2018) 426. https://doi.org/10.1016/j.ecolind.2018.03.041

24 S. N. Goward, and D. G. Dye: Adv. Space Res. **7** (1987) 165. https://doi.org/10.1016/0273-1177(87)90308-5

25 P. Maisongrande, A. Tuimy, G. Dedieu, and B. Saugier: Tellus B: Chem. Phys. Meteorol. **47** (1995) 178. https://doi.org/10.3402/tellusb.v47i1-2.16039

26 G. Asrar, M. Fuchis, E. T. Kanemasu, and J. L. Hatfield: Agron. J. **76** (1984) 300 https://doi.org/10.2134/agronj1984.00021962007600020029x